Computers and Electrical Engineering 102 (2022) 108243

Contents lists available at ScienceDirect

Computers and Electrical Engineering

journal homepage: www.elsevier.com/locate/compeleceng

A proactive Medium Access Control (MAC) for finite-sized machine-to-machine (M2M) communication networks☆

Adnan Fazil [a,*], Aamir Hasan [b], Bahman R. Alyaei [c], Khurram Khan [a], Muhammad Zakwan [a]

[a] Department of Avionics Engineering, Air University, E-9, Islamabad 44000, Pakistan
[b] Dhanani School of Science & Engineering, Habib University, Karachi 75290, Pakistan
[c] Department of Electrical and Computer Engineering, Air University, E-9, Islamabad 44000, Pakistan

ARTICLE INFO

Keywords:
Medium Access Control (MAC)
Machine-to-machine
Ad Hoc networks
Guard-zone
Interference suppression
Transmission capacity

ABSTRACT

In order to establish communication links among different communication devices or machines, the Medium Access Control (MAC) has to schedule the simultaneous transmissions by the contending nodes to constrain the probability of outage at each receiver. An efficient channel access scheme should be able to schedule the highest number of concurrent transmissions while being easy to implement with minimal coordination between the contending nodes.

The existing MAC schemes provide network-wide solutions without adaptiveness, such as in existing guard zone-based solutions. On the other hand, an adaptive channel access scheme is proposed in this paper, which instead of declaring a network-wide fixed guard zone employs each interferer's Transmitter–Receiver (Tx–Rx) separation to conclude its incorporation in the scheduled transmissions. The suggested scheme warrants the spatial separation among the scheduled links by suppressing the dominant interferers. The proposed MAC design functions approximately as good as the centralized, otherwise infeasible, joint scheduling and power control algorithm. In addition, the recommended scheme has proved its strength by outperforming both Carrier Sense Multiple Access (CSMA) and fix-sized guard zone schemes by significant margins under strict outage constraints and high contention density. The proposed scheme provided up to 100% and 60% better transmission capacity when compared with CSMA and fix-sized guard zone-based scheme, respectively. This paper also presents the closed-form results for the optimal guard zone size multiplier and the corresponding throughput capacity in terms of various network variables, such as contention density, outage constraint, Tx–Rx separation, network's path loss exponent and spreading factor.

1. Introduction

Since the inception of wireless communication technology, different techniques and applications to utilize wireless communication systems have always been a hot topic for researchers. One of the applications is the ad hoc network, which does not need any infrastructure and can be developed, on the go, by mutual cooperation between different wireless communication devices. Moreover, the ad hoc network is the building block for many emerging technologies, like Machine-to-Machine (M2M) communication and the

☆ This paper is for regular issues of CAEE. Reviews processed and recommended for publication to the Editor-in-Chief by Guest Editor Guanglong Du.

* Corresponding author.
E-mail addresses: adnan.fazil@mail.au.edu.pk (A. Fazil), aamir.hasan@sse.habib.edu.pk (A. Hasan), bahman@mail.au.eu.pk (B.R. Alyaei), khurram.jadoon@mail.au.edu.pk (K. Khan), mzakwan@mail.au.edu.pk (M. Zakwan).

https://doi.org/10.1016/j.compeleceng.2022.108243
Received 1 March 2021; Received in revised form 26 May 2022; Accepted 15 July 2022
Available online 5 August 2022

Internet of Things (IoT). Owing to their uncountable benefits and potential applications, ad hoc networks have been a key area of research for the last two decades and researchers have devised various useful algorithms to improve the network's throughput.

The research community is concentrating on a network with a large number of densely packed communication devices with shorter communication links by integrating different communication technologies and using smaller cells in cellular networks [1–3], which has a potential application in IoT. Nowadays, every human has one or more digital communication devices, and therefore, the need for a network with high throughput capacity is inevitable. Consequently, a lot of work has been done to improve the network's throughput or transmission capacity [4–8]. The research community is also working towards an M2M communication network with efficient Medium Access Control (MAC) layer, which not only packs the maximum number of transceivers into the network but also ensures an efficient energy consumption [9,10].

The M2M networks require an efficient MAC protocol that can be implemented in a distributed manner i.e. without network-wide Channel State Information (CSI) or signaling. An efficient MAC should achieve the best compromise between SINR and spatial reuse because packing more nodes in the network also increases the network's aggregate interference. Moreover, the protocol should be robust against the outages due to the dominant interferer. Hence, the research community has been in the pursuit of an optimal MAC protocol for distributed wireless networks [11–17].

1.1. Related work

An optimal scheduling scheme exists which schedules the contending nodes and also provides a power vector for optimal power transmission assignment to each of the scheduled transmitters [18]. However, this scheme is not practically implementable in a distributed network without network-wide CSI or centralized controller. Moreover, the assignment of minimum possible transmission power to the scheduled nodes restricts the inclusion of more transmitters in a densely packed, existing network. Another joint scheduling and power control scheme was proposed for ad hoc networks in [19]. However, this study considered some nodes to be master nodes, which act like the centralized controllers for groups of nodes and, therefore, the network model is not a pure, distributed ad hoc network.

There are different types of MAC protocols for wireless networks with respect to the working principles of the protocols and the supported network, such as centralized networks and distributed networks [20,21]. In this research, a distributed ad hoc network is considered for M2M communication unlike the cellular or centralized network-based M2M communication [22–25]. There are two major types of MAC protocols for distributed networks, contention-free protocols and contention-based protocols. In contention-free protocols such as TDMA [26,27], the devices need perfect synchronization that requires extra time and hardware. Moreover, contention-free protocols may be required based on the applications, such as in tactical networks where every node must have a dedicated channel or slot for communication [28]. However, such a MAC may lead to resource wastage when other MAC protocols can be used to optimize the resource allocation to enhance overall throughput [29].

On the other hand, the contention-based protocol maximizes the efficient use of the available resources to enhance the network's overall traffic carrying capacity while employing some Collision Resolution Algorithm [21]. Moreover, contention-based protocols such as Carrier Sense Multiple Access with Collision Avoidance (CSMA/CA) are widely used for ease of implementation and consequent flexibility. However, the probability of collision is proportional to the network size or node density, and the contention-based protocols do not scale well for very large or dense networks. Recently, some hybrid MAC protocols have also been proposed for M2M communication, but the network models for those protocols were either based on cellular networks or some of the contending nodes were considered to have some extra information/privilege [30–34] that contradicts with the definition of a purely distributed network. Therefore, as the purpose of this research is to maximize the overall throughput of the network, and the network model (explained later) is a finite-sized network, this paper focuses on the contention-based MAC protocols for the proposed scheme as well as for the comparison benchmarks.

The authors in [35] proposed a scheduling protocol for a Code Division Multiple Access (CDMA) based ad hoc network, but without a significant performance analysis with the existing schemes especially in terms of the spatial reuse. Moreover, they have not analyzed the ability of their protocol to retain the existing communication links while including more nodes in an established network. The authors used a stochastic model in [36] to optimize an ad hoc network's throughput by proposing a distributed scheduling algorithm that maximized the spatial reuse by introducing random sized guard zones around each active node. The scheme was not practically useful owing to its high probability of transmission collisions and outages, which results in poor resource management. A multistage contention-based protocol [37] was implemented in a distributed manner which achieved promising results. However, the network model assumed fixed Tx–Rx separations without utilizing any power control scheme.

The CSMA/CA is the underlying channel access scheme for IEEE 802.11 and is widely used for Wireless Local Area Network (WLAN) [38], and can be implemented in a distributed manner. However, the scheme has some inherent issues, such as hidden node and exposed node problems, owing to its algorithm that introduces a virtual exclusion zone around an active transmitter to safeguard that transmitter from the nearby interferers. On the other hand, a receiver should be safeguarded from interference to maximize the received SINR or probability of successful reception. Consequently, the CSMA scheme was outperformed by a distributed scheduling scheme which introduces exclusion zones around active receivers to inhibit the nearby interferers [39].

After the presentation of phenomenal concepts in [40], many researchers contemplated the concept of a receiver guard zone to notably enhance the network's transmission capacity [15,38,41]. Authors in [15,39] proved the efficacy of the receiver guard zone-based scheduling that outperformed the existing schemes. However, these studies were aimed to enhance the transmission capacity through inhibition of the nearby interfering transmitters, which are still believed to play a vital role in defining the network's overall

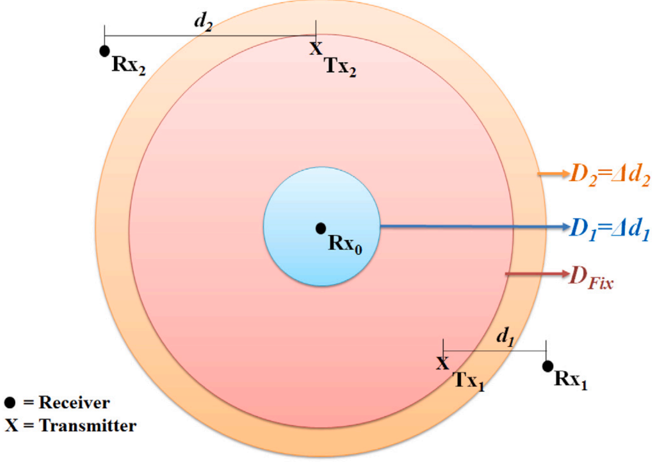

Fig. 1. An example to show that the closest interferer is not always the strongest interferer and therefore the network-wide fixed guard zone size (D_{Fix}) is not the best choice for interference suppression while maximizing the transmission capacity.

transmission capacity [42–44]. Therefore, the literature only proposed a fix-sized guard region around each receiver in the network to inhibit the interferers, irrespective of the interferer's transmission power or Tx–Rx separation.

The scholars in [39] proposed a network-wide fixed guard zone size for each receiver in an infinite-sized network with fixed Tx–Rx separations, under some outage constraint. Later, the authors in [15] considered a finite-sized ad hoc network with variable Tx–Rx separations and emphasized the significance of an adaptive guard zone. However, they again proposed and derived a fix-sized guard region around each receiver in the network to inhibit the interferers around a receiver, irrespective of the interferers' transmission power or Tx–Rx separations. On the other hand, we have proposed and derived an adaptive guard zone for a finite-sized network. As the transmission power by any interferer is proportional to its Tx–Rx separation, the proposed scheme makes the decision regarding an interferer's inclusion in the network based on its Tx–Rx separation, in addition to its distance from the subject receiver. In this way, the proposed scheme utilizes an adaptive guard zone that adapts to the interferer's transmission power. The suggested scheme admits the contending nodes in a sequence and accepts any new coming node if and only if it is not violating any existing, already scheduled node's corresponding guard zone which depends on the interferer's Tx–Rx separation.

1.2. Contributions

Under the Pairwise Power Control, any interferer's transmission power is a function of the interferer's own Tx–Rx separation and, therefore, the closest transmitter is not guaranteed to be the strongest or worst interferer. For example, let us suppose that there are two active transmitters i.e. Tx_1 and Tx_2 at a same distance from an active receiver (Rx_o). Now, under the pairwise power control, Tx_1 is transmitting $P_1 = \rho(d_1)^\alpha$ to Rx_1, which is at a distance d_1. Whereas, the second transmitter Tx_2 is transmitting $P_2 = \rho(d_2)^\alpha$ to Rx_2, which is at a distance d_2, as shown in Fig. 1.

In this scenario, if $d_2 = 2 \times d_1$ then $P_2 = 16 \times P_1$ for a moderate value of the path-loss exponent i.e. $\alpha = 4$, as per the definition of pairwise power control [45]. Although Tx_1 and Tx_2 are at the same distance from the subject receiver, the interference from Tx_2 is 16 times more powerful as compared to that of Tx_1. Consequently, Tx_1 might be able to transmit simultaneously without creating outages at Rx_o. Rationally, it is remarkably unreasonable to restrain both the interferers with a relatively large, fix-sized guard zone (D_{Fix}) proposed by [15,39]. Therefore, this paper suggests that an adaptive guard zone of size (radius) $D = \Delta \times d_t$ should be employed to repress the interfering transmitter with Tx–Rx distance of d_t, where Δ is the network-wide guard zone size multiplier or simply guard zone multiplier and its optimal value (Δ^*) needs to be found to render the maximum transmission capacity under some outage constraint. Therefore, under the proposed scheme, Tx_1 should be restrained if it falls within its corresponding guard zone (i.e. D_1) and similarly Tx_2 should be restrained if it violates its own corresponding guard zone (i.e. D_2), as shown in Fig. 1.

In an ad-hoc network, an efficient transmission scheduling scheme is mandatory for different communication links to co-exist in spatial proximity to enhance the spatial reuse [46–50]. Admittedly, various channel access strategies would perform differently with respect to major performance parameters; such as transmission capacity, Quality of Service (QoS), delays, probability of failed transmissions, energy consumption etc, under the exact same network model. However, our main objective in this paper is to develop a channel access scheme that maximizes the network's spatial reuse while meeting the outage constraint.

The remainder of the article is organized as follows. Section 2 explains the network model and assumptions considered in this study. Section 3 explains the suggested medium access and power control strategy as well as the derivation of an optimal value for the guard zone multiplier parameter (Δ^*), in terms of some major network characteristics, including the contention density. After that, the detailed analysis of the derived optimal guard zone multiplier and the corresponding transmission capacity has been performed in Section 4. Subsequently, a detailed performance comparison of the proposed scheme with the other well-known benchmarks, such as Joint Scheduling and Power Control Algorithm (JSPCA), CSMA and the fix-sized guard zone scheme [15,39] has been performed in Section 5 through extensive network simulations of all of these schemes. The distributed implementation of the proposed scheme is discussed with reference to the benchmark scheme in Section 6. In the end, the study is concluded in Section 7.

2. Network model

In this study, we have considered a wireless ad hoc network of large but finite radius R on a Two Dimensional (2D) plane, where N transmitters are uniformly distributed according to a Homogeneous Poisson Point Process (HPPP) with a spatial density of λ_o ($nodes/m^2$). Each transmitter (Tx) has its intended receiver (Rx), uniformly distributed in a disc of radius d_{max}, centered at that Tx. Consequently, the probability density function of Tx–Rx separations in the network is $f(x) = \frac{2x}{d_{max}^2}$.

As explained in the preceding section, the proposed design uses the guard zone criteria to decide on a transmitter's incorporation into the network and eventually picks a scheduled subset out of initially contending (N) transmitters, which can communicate simultaneously under the proposed spatial scheduling scheme. The proposed algorithm is sub-optimal in the sense that it does not search for the best or largest subset for scheduling and rather analyze the Tx–Rx pairs in a sequence to schedule the transmissions. However, this has been done because the selection of the best subset is not practically possible in a distributed network with a large number of contending nodes and, therefore, the nodes are arranged in a random sequence to start analyzing them under the guard zone criteria. Moreover, this random sequence of nodes may portray the priority of communication or generation of data at each transmitter in the wireless network, which is naturally random.

3. The optimal guard zone multiplier for a finite-sized network

An optimal guard zone should be the best compromise between the spatial reuse and the average probability of outage at each receiver, therefore, the derivation of an optimal guard zone or the guard zone multiplier has to fulfill two constraints i.e. the outage constraint and the spatial constraint. All the initially contending transmitters can transmit simultaneously but the simultaneous transmission will inevitably create huge interference at each receiver especially at higher density of contending nodes. Therefore, a constraint on the average probability of outage at each receiver should be defined to maintain the Quality of Service (QoS). Under the outage constraint, the average probability of outage at each active receiver should be less than some constraint ϵ. On the other hand, under the spatial constraint or the proposed spatial scheduling, each active receiver should be at a sufficient distance from all the interfering nodes. Consequently, the optimal guard zone multiplier i.e. Δ^* should be the best compromise between these two constraints to maximize the overall transmission capacity.

3.1. Maximum transmission capacity under the outage constraint

The results for the maximum possible density of active transmitters under some outage constraint were derived in [15] for a network on an infinite 2D plane with a fix-sized guard zone around the subject receiver. In this study, the radius of the network is R instead of infinity (∞) and the guard zone radius is $D = \Delta d_i$, where d_i is the interferer's Tx–Rx separation.

If a receiver (Rx_o) is placed at the origin and receiving ρ from its intended transmitter, under the PPC, then the probability of outage at Rx_o i.e. P_{out} can be written as (1)

$$P_{out} = P\left[\frac{\rho}{Mn + \sum_{i=1}^{N} \rho(d_{ii}/d_{io})^{\alpha}} < \frac{\gamma^*}{M}\right] \tag{1}$$

where n is the inherent noise at each receiver, d_{ii} is the Tx–Rx separation of the ith Tx–Rx pair, d_{io} is the separation between ith Tx (Tx_i) and Rx_o (i.e. origin), γ^* is the minimum SINR required for successful communication and M is the spreading gain of Direct Sequence CDMA (DS-CDMA). Now, if we introduce the proposed guard zone of radius $D = \Delta d_{ii}$ to inhibit Tx_i, then each interferer will be inhibited depending on its own Tx–Rx separation (d_{ii}) and its distance (d_{io}) from the origin (Rx_o). In this scenario, the probability of outage at Rx_o would be P_{out}^{GZ}, where

$$P_{out}^{GZ} = P\left[\frac{\rho}{Mn + \sum_{i\in(d_{io}>\Delta d_{ii})}^{N} \rho(\frac{d_{ii}}{d_{io}})^{\alpha}} < \frac{\gamma^*}{M}\right] \tag{2}$$

As per the outage constraint's definition, the probability of outage at the typical receiver should not exceed some constant ϵ. Therefore, we can formulate this constraint as in (3), which can be written as (4), where $\delta = \frac{1}{\gamma^*} - \frac{n}{\rho}$, and $Z = \sum_{i\in(d_{io}>\Delta d_{ii})}^{N}(\frac{d_{ii}}{d_{io}})^{\alpha}$ is the normalized (byρ) aggregate interference at the origin after proposed guard zone's implementation.

$$P\left[\frac{\rho}{Mn + \sum_{i\in(d_{io}>\Delta d_{ii})}^{N} \rho(\frac{d_{ii}}{d_{io}})^{\alpha}} < \frac{\gamma^*}{M}\right] \leq \epsilon \tag{3}$$

$$P[Z > M\delta] \leq \epsilon \tag{4}$$

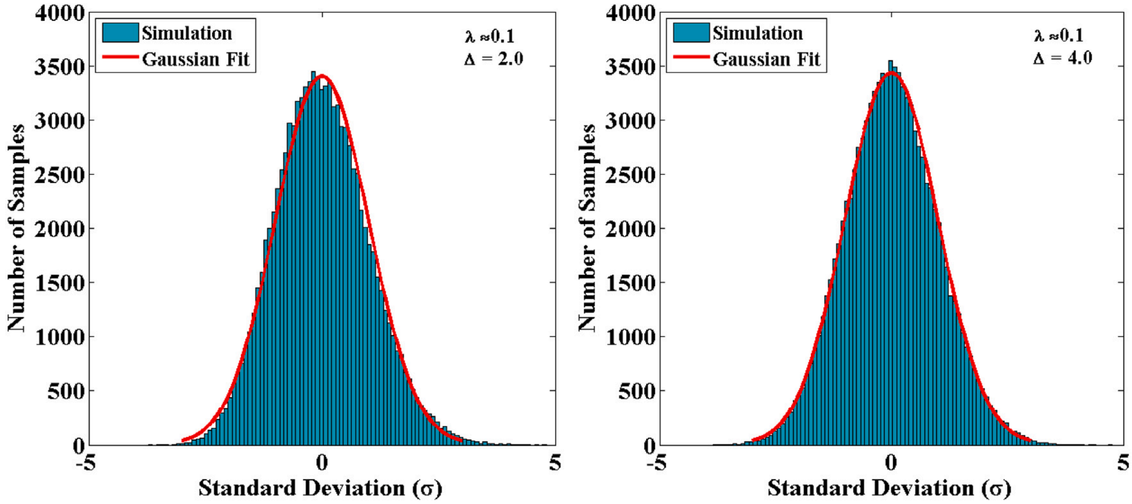

Fig. 2. Interference distribution at origin under simulation of the described system model compared with the Gaussian distribution, under different guard zone radii.

After using the Campbell's theorem, for $\alpha > 2$, we can find mean μ_z (5) and variance σ_z^2 (6) of the normalized aggregate interference (Z) after proposed guard zone's implementation around Rx_o. As evident from the equation, this expression takes into account the radius of the wireless network instead of integrating the interference from the infinite number of nodes as in [15].

$$\mu_z = E[Z(\lambda, \Delta)] = \frac{4\pi d_{max}^{\alpha} R^{2-\alpha}\lambda}{(2-\alpha)(2+\alpha)} - \frac{\pi d_{max}^2 \Delta^{2-\alpha}\lambda}{2-\alpha} \tag{5}$$

$$\sigma_z^2 = E[Z^2(\lambda, \Delta)] = \frac{\pi d_{max}^{2\alpha} R^{2-2\alpha}\lambda}{1-\alpha^2} - \frac{\pi d_{max}^2 \Delta^{2-2\alpha}\lambda}{2-2\alpha} \tag{6}$$

First, the probability density function of Z needs to be found to utilize the derived mean and variance to further derive the optimal value of the guard zone multiplier parameter i.e. Δ^*. The closed-form expression for Z was only found for a network with the fixed Tx–Rx separations without any guard zone [51]; nevertheless, we know that after inhibition of the nearby interferers, the distribution of the aggregate interference from farther nodes can be approximated by Gaussian distribution [52]. Therefore, the $Z's$ distribution is assumed to be Gaussian, which is backed by [52] and our simulation for the described system model in Fig. 2. Moreover, this assumption has also been verified through different simulations (shown in later sections). Thus, outage constraint of (4) can be rewritten as (7).

$$Q\left(\frac{M\delta - \mu_z}{\sigma_z}\right) \leq \epsilon \tag{7}$$

The maximum density of nodes ($\lambda_{out} = \lambda_{out}^{finite}$) that can communicate concurrently under given outage constraint can be found by substituting (5) and (6) in (7), which leads to (8), where $\Theta_1 = \frac{4\pi d_{max}^{\alpha} R^{2-\alpha}}{(2+\alpha)(2-\alpha)}$, $\Theta_2 = \frac{\pi d_{max}^2}{2-\alpha}$, $\Theta_3 = \frac{\pi d_{max}^{2\alpha} R^{2-2\alpha}(Q^{-1}(\epsilon))^2}{1-\alpha^2}$ and $\Theta_4 = \frac{\pi d_{max}^2 (Q^{-1}(\epsilon))^2}{2-2\alpha}$. On the other hand, the derivation of λ_{out} for an infinite sized 2D network, such as in [53], with same homogeneous node distribution and guard zone based scheduling leads to (9), where $\theta_1 = \frac{\pi d_{max}^2}{\alpha-2}$ and $\theta_2 = \sqrt{\frac{\pi}{2\alpha-2}}\, d_{max} Q^{-1}(\epsilon)$.

$$\lambda_{out}^{finite} = \frac{\Theta_3 - \Theta_4\Delta^{2-2\alpha}}{4(\Theta_1 - \Theta_2\Delta^{2-\alpha})^2}\left[\sqrt{1 + \frac{4M\delta(\Theta_1 - \Theta_2\Delta^{2-\alpha})}{\Theta_3 - \Theta_4\Delta^{2-2\alpha}}} - 1\right]^2, (\alpha > 2) \tag{8}$$

$$\lambda_{out}^{infinite} = \left[\frac{\theta_2}{2\theta_1\Delta}\left(\sqrt{1 + \frac{4\theta_1\delta\Delta^{\alpha}M}{\theta_2^2}} - 1\right)\right]^2, (\alpha > 2) \tag{9}$$

Eqs. (8) and (9) were compared by simulating the described system model and getting Δ^* against each value of N. Then these values of the optimal guard zone multiplier were used to calculate and plot λ_{out}^{finite} i.e. (8) and $\lambda_{out}^{infinite}$ i.e. (9) for different network parameters, as shown in Fig. 3. This comparison evidenced that (9) is a valid approximation for (8), and can also be utilized for the finite-sized WANETs. This occurs because the faraway transmitters in an infinite network have a negligible or almost zero probability of causing a blackout at a farther receiver.

3.2. Maximum transmission capacity under the spatial constraint

The suggested MAC design determines the scheduled nodes by examining all the nodes from 1 through N, only on the grounds of proposed guard zone criteria. The first Tx is always welcomed in the network because there is no other node to interfere with

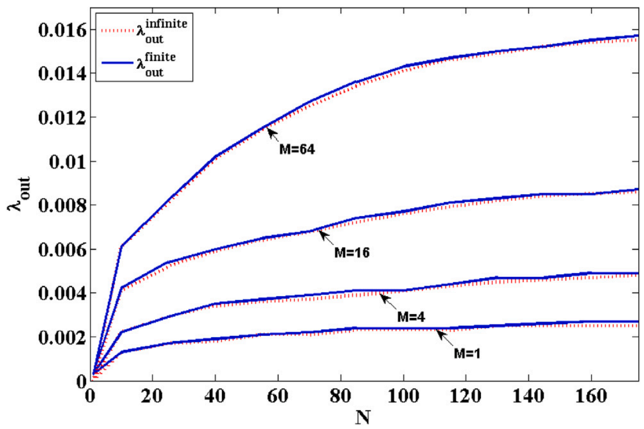

Fig. 3. Maximum allowed node density (λ_{out}) vs. Number of contending nodes (N), under some probability of outage (ϵ). These results were verified for different values of ϵ but only plotted here for $\epsilon = 0.01$. It is clear that the values for $\lambda_{out}^{infinite}$ are also applicable to the finite sized WANETs, under the given system model.

the first Tx–Rx pair. On the other hand, the 2nd Tx–Rx pair is accepted by the scheduling scheme if and only if the 1st and 2nd transmitters are not violating the guard zones of the 2nd and 1st receivers, respectively. If we assume that the scheduling scheme has tested i Tx–Rx pairs and has accepted l Tx–Rx pairs out of these i pairs, then at the subsequent step the system will test $(i+1)$th pair and will accept the pair if and only if the following two requirements are fulfilled:

1. $(i+1)$th *transmitter does not violate the guard zone of any of the* l*, already scheduled receivers.*
2. *Any of the* l*, already scheduled transmitters does not violate the guard zone of the* $(i+1)$th *receiver.*

The scheme will discard any Tx–Rx pair which is found to be disrupting the already accepted/scheduled pairs. After examining all the N initially contesting pairs in this way, the scheme will provide a subset of N_s^N scheduled nodes that fulfill the proposed scheduling criteria and can transmit simultaneously. The distribution of all the scheduled nodes is assumed to be Homogeneous Poisson, which will be validated through simulations in the subsequent sections. Under this Poisson assumption, the probability of acceptance for a pair given that l pairs have already been accepted, can be written as $p_l = e^{\frac{-2l\pi D^2}{\pi R^2}} = e^{\frac{-2lD^2}{R^2}}$, where D is the guard zone radius.

In this paper, the proposed guard zone is not a system-wide fixed guard zone like in [15] and, therefore, the expected value of the proposed guard zone's radius is used to assess D^2. Nevertheless, this assumption will also be validated through simulations in the subsequent sections. Utilizing the fact that the Tx–Rx separation under the given network model is distributed as $f(x) = \frac{2x}{d_{max}^2}$, the expected value for the square of the proposed guard zone's radius can be written as (10), where Δ is the network-wide fixed guard zone size multiplier. Consequently, for the proposed scheduling scheme, the probability of accepting a pair given that l pairs have already been accepted can be written as $p_l = e^{\frac{-l\Delta^2 d_{max}^2}{R^2}} = (e^{\frac{-\Delta^2 d_{max}^2}{R^2}})^l = (p)^l$, where p can be written as (11).

$$D^2 = \frac{\Delta^2 d_{max}^2}{2} \tag{10}$$

$$p = e^{\frac{-\Delta^2 d_{max}^2}{R^2}} \tag{11}$$

This acceptance of nodes, one at a time after analyzing a random number of contending nodes is similar to a geometric random variable, as in [15]. Moreover, the number of nodes that need to be tested to schedule each node of the scheduled network forms an independent geometric random variable and the average number of nodes to be tested to schedule that node corresponds to the mean of that geometric random variable. Therefore, the number of Tx–Rx pairs that can be scheduled successfully under the proposed scheduling scheme (i.e. N_s^N) out of the initially contending N Tx–Rx pairs can be found by putting the expected value of the N_s^Nth arrival time equal to N. Consequently, the maximum number of Tx–Rx pairs that can be scheduled (out of the initially contending N pairs) under the proposed, variably-sized guard zone scheme are derived to be (12). To validate the derived expression for N_s^N, the network was simulated and the simulation results were found for N_s^N, under different values of Δ or p. The results are plotted in Fig. 4, which show that Eq. (12) is a valid approximation for the number of successfully scheduled Tx–Rx pairs under the proposed scheme. Moreover, the difference in the derived and simulated values is because of the approximation made during the calculation of the void probability. The proposed guard zone is a variable-sized guard zone whose size/radius changes with the interferer's Tx–Rx separation; however, the void probability is calculated by approximating the size of the proposed guard zone with its expected value.

$$N_s^N = \frac{R^2}{\Delta^2 d_{max}^2} \ln[N(e^{\frac{\Delta^2 d_{max}^2}{R^2}} - 1) + 1] \tag{12}$$

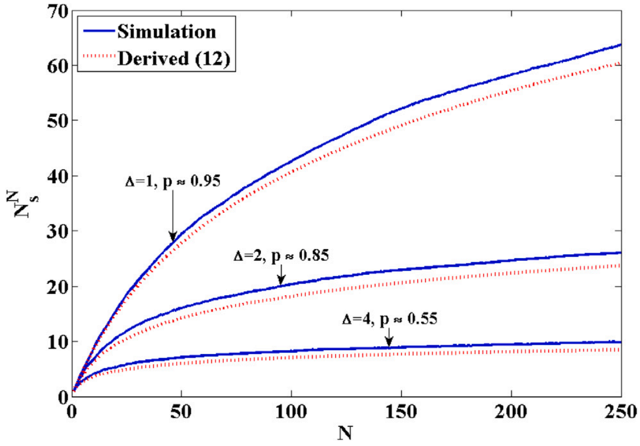

Fig. 4. Simulated and derived number of Tx–Rx pairs (N_s^N) vs. Number of contending nodes (N), under the spatial constraint. It is evident from the plots that the derived expression is a valid expression for the number of scheduled nodes under the spatial constraint of the proposed, adaptive guard zone.

Therefore, the intensity of nodes that can be scheduled under the spatial constraint can be written as (13).

$$\lambda_s = \frac{1}{\pi \Delta^2 d_{max}^2} \ln[N(e^{\frac{\Delta^2 d_{max}^2}{R^2}} - 1) + 1] \tag{13}$$

3.3. Optimal guard zone multiplier (Δ^*) and the corresponding transmission capacity (λ^*)

We have defined, formulated and derived two different constraints i.e. Outage Constraint and Spatial Constraint. The aim is to find the maximum possible (optimal) density of nodes that can communicate simultaneously (λ^*) and derive the corresponding optimal value of the guard zone multiplier parameter (Δ^*). Consequently, we have to solve the nonlinear optimization problem (14), where λ_o is the intensity of the contending nodes, λ_s is the derived spatial constraint and λ_{out} is the derived outage constraint (i.e. $\lambda_{out}^{infinite}$). The solution of (14) is the intersection of λ_s and λ_{out} when plotted against the guard zone radius. As we know that λ_s decreases with an increase in the guard zone size or Δ, and λ_{out} is proportional to Δ, the intersection is bound to occur. Therefore, the optimal value of Δ i.e. Δ^* was derived by putting $\lambda_{out} = \lambda_s$ and solving for Δ.

$$\lambda(\Delta) = \max_{\Delta,\lambda_o}[\min(\lambda_s, \lambda_{out})] \tag{14}$$

Consequently, simplifications after using (9), (13) and the results of [15] lead to the optimal value of the guard zone multiplier (15) and the corresponding transmission capacity (16) for a finite-sized DS-CDMA ad hoc network.

$$\Delta^* = \sqrt{\frac{12}{5\pi}} \left(\frac{Q^{-1}(\epsilon)}{M\delta}\right)^{\frac{1}{\alpha}} \left[\ln\left(1 + \frac{N d_{max}^2}{R^2}\left(\frac{Q^{-1}(\epsilon)}{M\delta}\right)^{\frac{2}{\alpha}}\right)\right]^{\frac{1}{2\alpha}} \tag{15}$$

$$\lambda^* = \frac{5}{12 d_{max}^2} \left(\frac{M\delta}{Q^{-1}(\epsilon)}\right)^{\frac{2}{\alpha}} \left[\ln\left(1 + \frac{N d_{max}^2}{R^2}\left(\frac{Q^{-1}(\epsilon)}{M\delta}\right)^{\frac{2}{\alpha}}\right)\right]^{\frac{\alpha-1}{\alpha}} \tag{16}$$

4. Optimal guard zone multiplier and corresponding transmission capacity's analysis

In this section, the analytical results i.e. the derived guard zone multiplier (15) and the corresponding optimal transmission capacity (16) are plotted against the number of contending nodes and path-loss exponent for different values of the spreading gain to investigate the impact of various network parameters on these values. Moreover, the results for Δ^* and λ^* from the extensive network simulations of the defined network model for the network parameters of Table 1 are also plotted to verify the hypotheses made during the derivation of (15) and (16). The simulated results are averaged over 1000 network realizations, and therefore, the error margin is 3.1% under the confidence level of 95%. These results not only validate the derived expressions but also validate the approximations and assumptions made during the derivation of these expressions.

4.1. Analysis of Δ^*

Fig. 5 presents the derived and simulated Δ^* against the number of contending nodes i.e. N, for four different values of spreading gain M, where $M = 1$ represents the narrow-band network. The plots show that the value of Δ^* is proportional to N; however, the change in Δ^* is not very notable for a major change in the number of contending nodes. This implies that the fixed Δ^* can

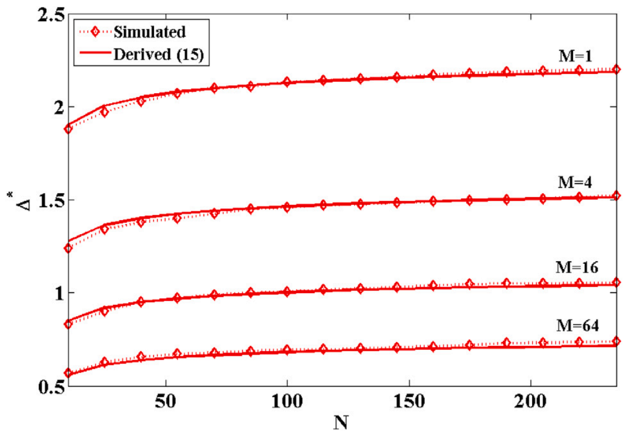

Fig. 5. Derived and simulated optimal guard zone multiplier (Δ^*), plotted against the number of contending nodes (N), for four different values of spreading gain (M). The spreading gain plays a vital role in determining the guard zone multiplier, which is inversely related to the spreading gain.

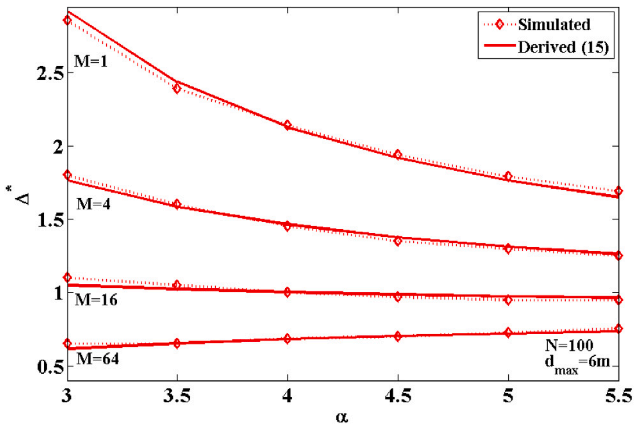

Fig. 6. Derived and simulated optimal guard zone multiplier (Δ^*), plotted against the network's path-loss exponent (α), for four different values of spreading gain (M). The multiplier is inversely related to the path-loss for smaller spreading gain, but the relationship changes at higher spreading gains.

Table 1
Network parameters, unless otherwise specified.

Symbol	Description	Value
R	Network radius	30 m
n	Receiver noise	0.001
ϵ	Outage constraint	0.01
α	Path loss exponent	4
γ^*	Minimum required SINR	10 dB
d_{max}	Maximum allowed Tx–Rx separation	6 m
M	Spreading gain	1

also provide significant transmission capacity over a wide range of N, as shown in [53] where the guard zone multiplier was not a function of N or λ_o. Moreover, the higher value of spreading gain supports a smaller guard zone because the SINR requirement decreases with an increase in the spreading gain, and the lower SINR requirement favors a smaller guard zone radius.

Similarly, Fig. 6 shows the derived and simulated Δ^* against the wireless network's path-loss exponent i.e. α, for four different values of spreading gain M, where $M = 1$ depicts the narrow-band network. The figure shows that the value of Δ^* decreases with α for a narrow band network and the networks with small spreading gain. However, Δ^* is proportional to α for very high spreading gain such as at $M = 64$. This change in the behaviors of Δ^* against α is possibly due to effect of the term $(\frac{Q^{-1}(\epsilon)}{M\delta})^{\frac{1}{\alpha}}$ in Eq. (15), because when $M\delta > Q^{-1}(\epsilon)$ the overall term increases with α. Moreover, the optimal guard zone multiplier i.e. Δ^* is almost insensitive to the path-loss exponent when $M\delta \approx Q^{-1}(\epsilon)$.

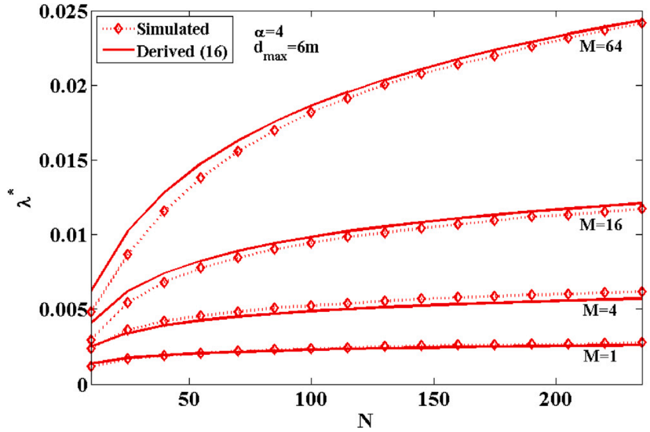

Fig. 7. Derived and simulated optimal transmission capacity (λ^*), plotted against the number of contending nodes (N), for four different values of spreading gain (M). The optimal transmission capacity is proportional to both the contention density and the spreading gain.

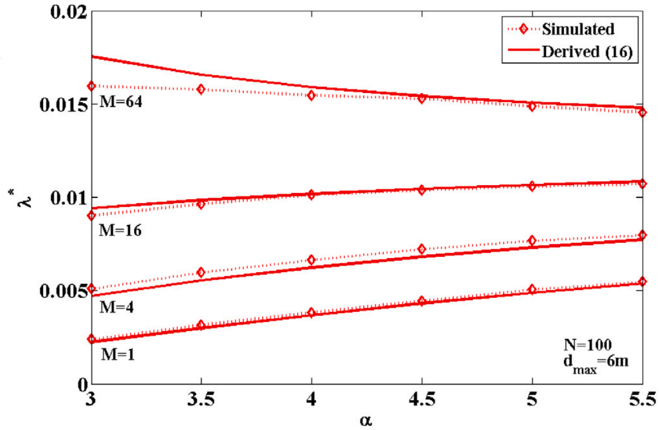

Fig. 8. Derived and simulated transmission capacity (λ^*) plotted against the network's path-loss exponent (α), for four different values of spreading gain (M). The optimal transmission capacity is proportional to the path-loss for smaller spreading gain, but the relationship changes at higher spreading gains.

4.2. Analysis of λ^*

Fig. 7 displays the derived and simulated λ^* against the number of contending nodes i.e. N, for four different values of spreading gain M, where $M = 1$ depicts the narrow-band network. The plots in this figure show that the transmission capacity (λ^*) is proportional to N. However, the transmission capacity increases linearly with N, only for the small numbers of initially contending nodes, and then saturates with a further increase in N, especially for a narrow-band network. This happens because, at lower intensities of contending nodes, the inherent separation allows a large percentage of contending nodes to be accepted by the proposed scheme and that percentage starts to decrease with the increasing intensity owing to densely packed contending nodes. On the other hand, higher spreading gain supports a smaller guard zone multiplier and allows the scheme to pack more nodes even at higher contention densities. In addition, it is evident that for any number of contending nodes the higher value of spreading gain provides a significant gain in transmission capacity, because it relaxes the SINR constraints and also permits more nodes to be packed by the scheme through a smaller guard zone radius.

In Fig. 8, the derived and simulated λ^* were also plotted against the path-loss exponent for four different values of the spreading gain (M), where $M = 1$ depicts the narrow-band network. It can be seen that the λ^* is proportional to α for a narrow band network and for the network with small spreading gain. However, it decreases with α for very high spreading gain such as at $M = 64$. This is again due to effect of the term $(\frac{M\delta}{Q^{-1}(\epsilon)})^{\frac{2}{\alpha}}$ in Eq. (16), because when $M\delta > Q^{-1}(\epsilon)$ the transmission capacity i.e. λ^* decreases with α. Moreover, like the Δ^*, λ^* is almost insensitive to α for $M\delta \approx Q^{-1}(\epsilon)$.

In addition, Eq. (16) shows that the transmission capacity decreases exponentially with increasing d_{max} because the larger Tx–Rx separations deteriorate the ability of the scheme to pack more nodes during the guard zone scheduling and also increase the aggregate interference under PPC.

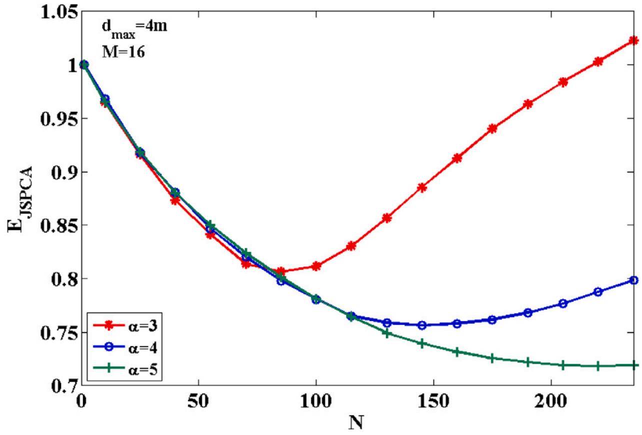

Fig. 9. The transmission efficiency (E_{JSPCA}) plotted against the number of initially contending transmitters N, for three different values of the path-loss exponent α.

5. Performance analysis and discussion

A detailed analysis of the proposed scheme's performance has also been carried out while making a comparison with the well-known existing schemes. As the derived expressions have already been validated through network simulations and the closed-form expressions of some of the benchmarks do not exist, the comparison was performed through extensive simulations of all the schemes where the considered benchmarks include Carrier Sense Multiple Access (CSMA) scheme, system-wide fixed exclusion zone scheme [15,39], and the centralized, Joint Scheduling and Power Control scheme. Each of the benchmarks along with the proposed scheme was simulated in MATLAB for the same network model, and the results were averaged over 2000 network realizations to get reliable results and smooth plots. As each value of the simulated results is an average of 2000 samples, therefore, the error margin is 2.2% under the confidence level of 95%.

5.1. Proposed scheme versus the near-optimal centralized scheme

An optimum joint scheduling and power control scheme for a channelized cellular communication network was proposed in [54,55] and the results were shown by [18] to be also applicable to the ad hoc networks, given that the nodes have network-wide CSI. As discussed earlier, the assumption of having global CSI to discover a subset of initially contending nodes that can transmit simultaneously is not possible in a distributed ad hoc network, and the scheme has only been simulated to highlight the strength of the proposed scheme when compared to an optimal, otherwise infeasible centralized scheme.

To comprehend the real gains of the proposed scheme's performance, its transmission capacity has also been compared with the centralized scheme by simulating a network for the provided system model, using the network parameters of Table 1. For each value of the number of initially contending nodes N, the proposed scheme and the centralized scheme were implemented on the same initial distribution to get the relative results. This process was repeated for a large number of iterations to get practical results, over a range of N. The transmission efficiency (E_{JSPCA}) of the proposed scheme is represented here as the ratio of the transmission capacity under the proposed scheme to the transmission capacity of the centralized, JSPCA scheme (17).

$$E_{JSPCA} = \lambda^*/\lambda_{JSPCA} \tag{17}$$

In Fig. 9, the efficiency is plotted against the number of initially contending Tx–Rx pairs (N) for three different values of the path-loss exponent (α). The plots show that the efficiency plummets to a minimum level and then begins to increase with the contention density, which in particular is a very unique result when compared to [15], where the efficiency kept on declining with the contention density. Furthermore, the higher path-loss provides greater efficiency in a sparsely distributed network, because the suggested scheme inhibits closely located nodes and the higher path-loss significantly attenuates the interference from sparsely distributed, distant interferes. Nevertheless, at larger contention densities, the lower path-loss exponent supports the proposed scheme by incorporating a bigger guard zone through a larger Δ^* to inhibit most of the closely placed interferers. In addition, the proposed scheme provides at least 75% efficiency at moderate values of N and α.

Fig. 9 also demonstrates that the proposed scheme can outperform JSPCA. This is because the near-optimal scheme is implemented here in a sub-optimal manner. After all, instead of searching for the largest possible subset of nodes, the nodes are tested/scheduled in a random sequence as explained earlier. This procedure has also been utilized by [15] for simulation and performance comparison of different benchmarks. Therefore, at higher contention density and lower path loss exponent, the proposed scheme has the potential to outperform the JSPCA as well.

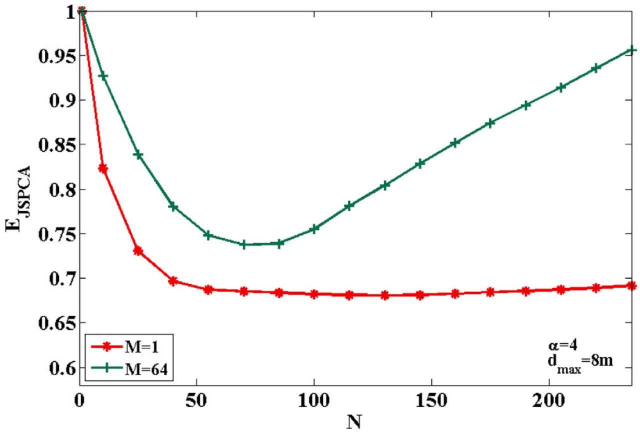

Fig. 10. The transmission efficiency (E_{JSPCA}) plotted against the number of initially contending transmitters N, for two different values of the spreading gain M.

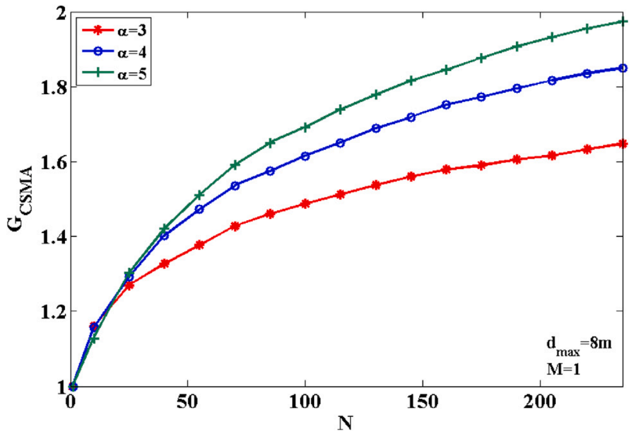

Fig. 11. The gain in the transmission capacity (G_{CSMA}) plotted against the number of initially contending transmitters N, for different values of path-loss exponent α.

Similarly, the performance is plotted against the number of originally contending Tx–Rx pairs (N) for two distinct values of spreading gain (M), in Fig. 10. It can be observed that for any value of N, the efficiency is proportional to the spreading factor because the higher spreading gain enables more nodes to transmit concurrently by employing a smaller guard zone or Δ^*. Moreover, the higher spreading gain enhances the degree of variation in the efficiency against the contention density.

5.2. Proposed scheme versus CSMA

The CSMA is the underlying channel access scheme for the widely used IEEE 802.11 [38] and therefore the proposed scheme's performance is also correlated to the well-known CSMA scheme to accentuate its strengths and benefits by simulating the CSMA scheme for the defined, finite network. The extensive network simulations confirmed that the proposed scheme provides a substantial increase in the transmission capacity when compared to the CSMA scheme. This gain in the capacity is expressed as (18), where λ_{CSMA} is the transmission capacity under the CSMA scheme.

$$G_{CSMA} = \frac{\lambda^*}{\lambda_{CSMA}} \tag{18}$$

In Fig. 11, the gain is plotted against the number of initially contending Tx–Rx pairs (N) for three different values of the path-loss exponent (α). The G_{CSMA} is proportional to N, because the CSMA algorithm, unlike the proposed scheme, is not able to perform efficiently in a network with densely packed nodes and consequently experiences blackouts. It is also apparent that the gain is not very sensitive to the network's path-loss at lower node densities, but the higher path-loss supports higher G_{CSMA} at higher values of N. As observed earlier, a higher path-loss is profitable for the proposed scheme and hence supports higher G_{CSMA}, because the higher path-loss maintains a smaller Δ^* and encourages the proposed scheme to schedule more transmitters in the network. Moreover, the suggested scheduling scheme provides almost 100% better transmission capacity as compared to the CSMA.

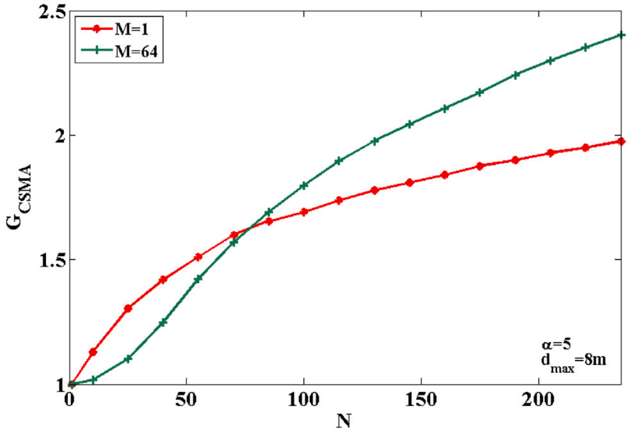

Fig. 12. The gain in the transmission capacity (G_{CSMA}) plotted against the number of initially contending transmitters N, for different values of spreading gain M.

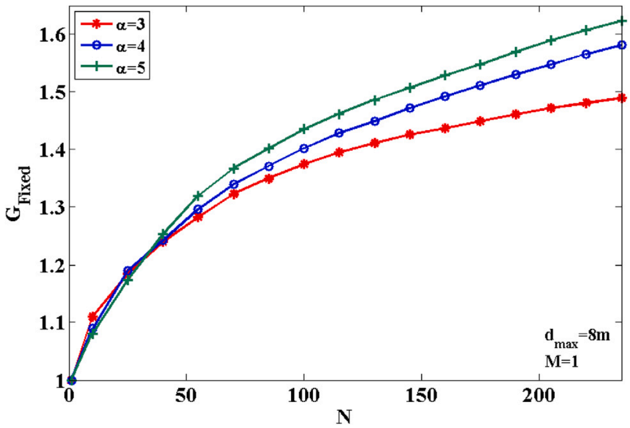

Fig. 13. The gain in the transmission capacity (G_{Fixed}) plotted against the number of initially contending transmitters N, for three different values of the path-loss exponent α.

In Fig. 12, the proposed scheme's gain with respect to CSMA is plotted versus the number of initially contending nodes (N), for two distinct values of spreading gain M. The plots attest that the gain decreases with the spreading gain at smaller values of N. On the other hand, at higher densities of initially contending nodes, the gain in transmission capacity corresponding to higher spreading gain outperforms the smaller spreading gains.

5.3. Proposed scheme versus fix-sized exclusion zone

A notable improvement in the transmission capacity was demonstrated by authors through system-wide fix-sized receiver guard-zones, both for infinite-sized and finite-sized networks with similar network models in [15,39], respectively. In a finite-sized network, the fix-sized guard zone evidenced a substantial growth in the transmission as well as in the transport capacity when compared to the other well-known scheduling schemes [15]. The proposed scheme's performance has also been compared to this distributed scheme's results through extensive simulations of the same network. The suggested design rendered a significant gain in the transmission capacity when correlated to the fix-sized exclusion zone. This gain in the transmission capacity is denoted by G_{Fixed} and defined as (19), where λ_{Fixed} is the transmission capacity under the fix-sized guard zone scheme.

$$G_{Fixed} = \frac{\lambda^*}{\lambda_{Fixed}} \tag{19}$$

After averaging over two thousand network realizations, the results are plotted against different network parameters to investigate the proposed scheme's robustness. In Fig. 13, the gain is plotted versus the number of initially contending Tx–Rx pairs (N) for three different values of the path-loss exponent (α). The gain, G_{Fixed} is proportional to N because the fix-sized guard zone is not as efficient in a network with densely packed nodes and inhibits some of the nodes through large guard zone size, which are otherwise scheduled by the proposed scheme. These plots also reveal that the gain is nearly insensitive to the network's path-loss

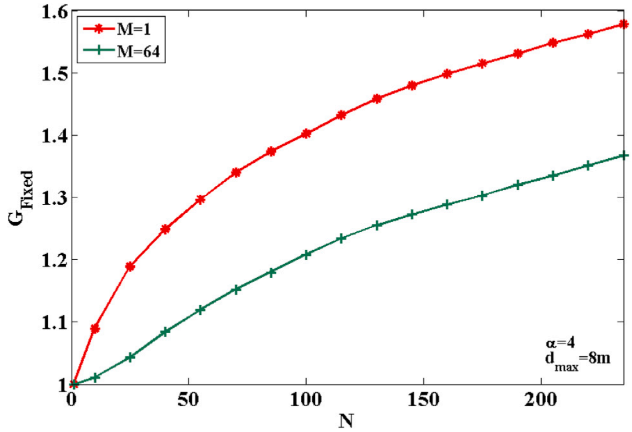

Fig. 14. The gain in transmission capacity (G_{Fixed}) plotted against the number of initially contending transmitters N, for two different values of spreading gain M.

Table 2
Proposed scheme's comparison with the benchmark MAC schemes.

MAC scheme	CSMA	Fix-sized guard zone	Proposed scheme
Category	Contention-based	Contention-based	Contention-based
Implementation	RTS/CTS Packets	RTS/CTS Packets	RTS/CTS Packets
Transmission capacity (λ^*)	0.005	0.00625	0.01
Transmission gain wrt CSMA	0%	25%–30%	100%–140%

exponent even over an extended range of N. Overall, the plots substantiate the proposed scheme's genuine strength by confirming that the fix-sized guard zone scheme's transmission capacity has been surpassed by almost 60%.

The impact of the spreading factor on the transmission gain has also been analyzed. In Fig. 14, the suggested scheme's gain is plotted against the number of initially contesting nodes (N) for two distinct values of spreading gain M. The plots show that the gain decreases with an increase in the spreading gain over all the values of N. This inverse relation is because of the higher spreading gain's ability to ease the SINR constraints and support the fixed guard zone scheme.

These results highlight the true strength of the proposed scheme when compared with the existing, fix-sized receiver guard zone-based scheduling scheme [15] for the same network model. Although [15] derived a network-wide fixed guard zone around each receiver in the network as a function of the number of initially contending Tx–Rx pairs, the proposed scheme is an adaptive scheduling scheme in the true sense because it derived a network-wide fixed guard zone multiplier which needs to be multiplied with the interferer's Tx–Rx separation to find the guard zone size/radius for inhibition of that specific interferer by any receiver.

6. Distributed implementation

In this paper, the performance of the proposed scheme has been compared with well-known existing scheduling schemes to demonstrate its actual strength. The proposed scheme's performance is better in the analyzed network model without an increase in the implementation complexity. Like [15], we consider that there are two non-overlapping frequency channels, one is the control channel and the other one is the data channel. The exchange of control packets over the control channel among different nodes will help the implementation of the proposed transmission scheduling and power control scheme. The control channel is a narrow band channel for short control packets whereas the data channel is using DS-CDMA at the physical layer. The virtual carrier sensing through Request-to-Send (RTS) and Clear-to-Send (CTS) control packets for implementation of fix-sized receiver guard zones in [15] will help in the efficient implementation of the proposed variable-sized receiver guard zone without any change or addition in the control packets. This fact has also been elaborated in the comparison presented in Table 2. The use of these control packets for the implantation of the proposed scheme is explained below.

6.1. Implementation of pairwise power control

The pairwise power control can be implemented as described in [15]. The control packets will be transmitted at the maximum available power and the received power at the receiver for the RTS packet can help the implementation of the power control scheme among different Tx–Rx pairs.

6.2. Implementation of proposed variable sized guard zone

To implement the fix-sized guard zone [15], the transmitters measure the power of received CTS packets transmitted by the active receivers and find out whether they are within the guard zone of an already scheduled receiver. The proposed scheme can be executed similarly where the transmitter (potential interferer) will monitor the received power of the CTS and therefore will find out its distance from the receiver who transmitted the CTS packet.

However, in the proposed scheme, the guard zone radius is a function of the interferer's Tx–Rx separation, as explained in Section 1.2. Therefore, the transmitter will also use its Tx–Rx separation (d_t) to find the guard zone radius ($D = \Delta^* \times d_t$) around a receiver for its inhibition or incorporation in the network. As each Tx–Rx pair knows its Tx–Rx separation, the spatial scheduling can be implemented with the same control packets that can implement the fix-sized guard zone scheme. Therefore, despite providing a significant gain in the network's overall transmission capacity, the proposed scheme can be implemented in a distributed manner without an increase in the complexity when compared with the existing distributed scheme [15].

7. Conclusion

In this paper, unlike the existing solutions, an adaptive guard zone based scheduling scheme is modeled for the finite-sized wireless ad hoc networks. The proposed scheme is employing scheduling and power control in an adaptive and distributed manner without network-wide information sharing among the nodes. The derivation resulted in a closed-form expression for a network-wide guard zone size multiplier, which is also validated through extensive network simulations.

The performance analysis of the proposed scheme clearly highlighted its superiority over the existing distributed scheduling schemes. Moreover, the scheme provides promising results when compared to a centralized, otherwise infeasible scheduling scheme for the explained network model. The proposed algorithm ensures adaptive guard zone around each active receiver which proved its strengths by providing significant i.e. greater than 100% and 60% gain in the transmission capacity when compared to the well known CSMA and the fix-sized guard zone scheme, respectively.

As proposed future research directions, the work can be further extended to Three Dimensional (3D) or Flying Ad Hoc Networks (FANETs). Moreover, the optimal guard zone multiplier may be derived and analyzed for similar network with nodes having directional antenna. Furthermore, the work can be extended for different node distributions and node mobility models for different future applications.

CRediT authorship contribution statement

Adnan Fazil: Conceptualization, Methodology, Software, Writing – original draft. **Aamir Hasan:** Conceptualization, Resources, Supervision. **Bahman R. Alyaei:** Formal analysis, Investigation. **Khurram Khan:** Validation, Visualization. **Muhammad Zakwan:** Writing – review & editing, Project administration.

Declaration of competing interest

No author associated with this paper has disclosed any potential or pertinent conflicts which may be perceived to have impending conflict with this work. For full disclosure statements refer to https://doi.org/10.1016/j.compeleceng.2022.108243.

References

[1] Abbasi M, Shahraki A, Barzegar HR, Pahl C. Synchronization techniques in "Device to device- and vehicle to vehicle-enabled" cellular networks: A survey. Comput Electr Eng 2021;90:106955. http://dx.doi.org/10.1016/j.compeleceng.2020.106955.
[2] Hwang I, Song B, Soliman SS. A holistic view on hyper-dense heterogeneous and small cell networks. IEEE Commun Mag 2013;51(6):20–7. http://dx.doi.org/10.1109/MCOM.2013.6525591.
[3] Alyaei BR, Qureshi IM, Saleem S, Abbassi SH. Offloading with hybrid cell association in non-uniform heterogeneous cellular networks: Modeling and performance analysis. IEEE Access 2019;7:172214–30. http://dx.doi.org/10.1109/ACCESS.2019.2955934.
[4] Gezer A, Okdem S. ☆Improving IEEE 802.15.4 channel access performance for IoT and WSN devices. Comput Electr Eng 2020;87:106745. http://dx.doi.org/10.1016/j.compeleceng.2020.106745.
[5] Ranjbar M, Tran NH, Vu MN, Nguyen TV, Gursoy MC. Capacity region and capacity-achieving signaling schemes for 1-bit ADC multiple access channels in Rayleigh fading. IEEE Trans Wireless Commun 2020;19(9):6162–78. http://dx.doi.org/10.1109/TWC.2020.3000610.
[6] Yilmaz F. On the relationships between average channel capacity, average bit error rate, outage probability, and outage capacity over additive white Gaussian noise channels. IEEE Trans Commun 2020;68(5):2763–76. http://dx.doi.org/10.1109/TCOMM.2020.2972328.
[7] Mammeri S, Yazid M, Kacimi R, Bouallouche-Medjkoune L. Starvation avoidance-based dynamic multichannel access for low priority traffics in 802.11ac communication systems. Comput Electr Eng 2021;90:106942. http://dx.doi.org/10.1016/j.compeleceng.2020.106942.
[8] Vinoth Kumar M, Ram RS, B. SB, Amutha B, Kowsigan M. An improved migration scheme to achieve the optimal service time for the active jobs in 5G cloud environment. Comput Commun 2020;160:807–14. http://dx.doi.org/10.1016/j.comcom.2020.06.014.
[9] Das SK, Hossain MF. A location-aware power control mechanism for interference mitigation in M2M communications over cellular networks. Comput Electr Eng 2020;88:106867. http://dx.doi.org/10.1016/j.compeleceng.2020.106867.
[10] Ali A, Shah GA, Shoaib M. Energy efficient uplink MAC protocol for M2M devices. IEEE Access 2019;7:35952–62. http://dx.doi.org/10.1109/ACCESS.2019.2903647.
[11] Tushar V, Sharma D. Device and method for scheduling machine-to-machine communication system. 2019.
[12] Bouzebiba H, Lehsaini M. A novel equilibrated scheduling algorithm for multimedia transmission in internet of multimedia things. Comput Electr Eng 2020;88:106863. http://dx.doi.org/10.1016/j.compeleceng.2020.106863.

[13] Cao S, Lee VCS. A novel adaptive TDMA-based MAC protocol for VANETs. IEEE Commun Lett 2018;22(3):614–7. http://dx.doi.org/10.1109/LCOMM.2017.2785378.

[14] Qiu L, Cao G. Popularity-aware caching increases the capacity of wireless networks. IEEE Trans Mob Comput 2019;1. http://dx.doi.org/10.1109/TMC.2019.2892419.

[15] Hasan A, Ali A. Guard zone-based scheduling in ad hoc networks. Comput Commun 2015;Complete(56):89–97. http://dx.doi.org/10.1016/j.comcom.2014.11.004.

[16] Das S, Pal S. Analysis of energy-efficient routing protocols in mobile ad hoc network. In: Biswas U, Banerjee A, Pal S, Biswas A, Sarkar D, Haldar S, editors. Advances in computer, communication and control. Lecture notes in networks and systems, Springer Singapore; 2019, p. 285–95.

[17] Kadam S, Prabhu D, Rathi N, Chaki P, Kasbekar GS. Exploiting group structure in MAC protocol design for multichannel ad hoc cognitive radio networks. IEEE Trans Veh Technol 2019;68(1):893–907. http://dx.doi.org/10.1109/TVT.2018.2883392.

[18] ElBatt T, Ephremides A. Joint scheduling and power control for wireless ad hoc networks. IEEE Trans Wireless Commun 2004;3(1):74–85. http://dx.doi.org/10.1109/TWC.2003.819032.

[19] Malekshan KR, Zhuang W. Joint scheduling and transmission power control in wireless ad hoc networks. IEEE Trans Wireless Commun 2017;16(9):5982–93. http://dx.doi.org/10.1109/TWC.2017.2717985.

[20] Rajandekar A, Sikdar B. A survey of MAC layer issues and protocols for machine-to-machine communications. IEEE Internet Things J 2015;2(2):175–86. http://dx.doi.org/10.1109/JIOT.2015.2394438.

[21] Sotenga PZ, Djouani K, Kurien AM. Media access control in large-scale internet of things: A review. IEEE Access 2020;8:55834–59. http://dx.doi.org/10.1109/ACCESS.2020.2982357.

[22] Alhussien N, Gulliver TA. Optimal resource allocation in cellular networks with H2H/M2M Coexistence. IEEE Trans Veh Technol 2020;69(11):12951–62. http://dx.doi.org/10.1109/TVT.2020.3016239.

[23] Zhang S, Chen M. Cluster formation and power control for M2M-enabled two-tier cellular network. In: 2018 IEEE 4th international conference on computer and communications (ICCC). 2018, p. 673–7. http://dx.doi.org/10.1109/CompComm.2018.8781006.

[24] Gu B, Zhang C, Wang H, Yao Y, Tan X. Power control for cognitive M2M communications underlaying cellular with fairness concerns. IEEE Access 2019;7:80789–99. http://dx.doi.org/10.1109/ACCESS.2019.2914157.

[25] Althumali HD, Othman M, Noordin NK, Hanapi ZM. Dynamic backoff collision resolution for massive M2M random access in cellular IoT networks. IEEE Access 2020;8:201345–59. http://dx.doi.org/10.1109/ACCESS.2020.3036398.

[26] Benrebbouh C, Louail L. Dynamic TDMA for wireless sensor networks. In: 2021 30th wireless and optical communications conference (WOCC). 2021, p. 204–8. http://dx.doi.org/10.1109/WOCC53213.2021.9602892.

[27] Jabandžić I, Giannoulis S, Mennes R, De Figueiredo FAP, Claeys M, Moerman I. A dynamic distributed multi-channel TDMA slot management protocol for ad hoc networks. IEEE Access 2021;9:61864–86. http://dx.doi.org/10.1109/ACCESS.2021.3074594.

[28] Wi G, Son S, Park K-J. Delay-aware TDMA scheduling with deep reinforcement learning in tactical MANET. In: 2020 international conference on information and communication technology convergence (ICTC). 2020, p. 370–2. http://dx.doi.org/10.1109/ICTC49870.2020.9289080.

[29] Olatinwo DD, Abu-Mahfouz AM, Hancke GP. Towards achieving efficient MAC protocols for WBAN-enabled IoT technology: A review. EURASIP J Wireless Commun Networking 2021;2021(1):60. http://dx.doi.org/10.1186/s13638-021-01919-1.

[30] Shu T, Krunz M. Energy-efficient power/rate control and scheduling in hybrid TDMA/CDMA wireless sensor networks. Comput Netw 2009;53(9):1395–408. http://dx.doi.org/10.1016/j.comnet.2009.01.006.

[31] Rozario AB, Hossain MF. Hybrid TDMA-NOMA based M2M communications over cellular networks with dynamic clustering and 3D channel models. In: 2019 international symposium on advanced electrical and communication technologies (ISAECT). 2019, p. 1–6. http://dx.doi.org/10.1109/ISAECT47714.2019.9069708.

[32] Li Z, Gui J. Energy-efficient resource allocation with hybrid TDMA–NOMA for cellular-enabled machine-to-machine communications. IEEE Access 2019;7:105800–15. http://dx.doi.org/10.1109/ACCESS.2019.2931657.

[33] Tan Z, Qu H, Zhao J, Ren G, Wang W. Self-sustainable dense cellular M2M system with hybrid energy harvesting and high sensitivity rectenna. IEEE Access 2019;7:19447–60. http://dx.doi.org/10.1109/ACCESS.2019.2897115.

[34] Ázquez-Gallego FV, Alonso-Zarate J, Balboteo I, Alonso L. DPCF-M: A medium access control protocol for dense machine-to-machine area networks with dynamic gateways. In: 2013 IEEE 14th workshop on signal processing advances in wireless communications (SPAWC). 2013, p. 490–4. http://dx.doi.org/10.1109/SPAWC.2013.6612098.

[35] Muqattash A, Krunz M. CDMA-based MAC protocol for wireless ad hoc networks. In: Proceedings of the 4th ACM international symposium on mobile ad hoc networking & computing. MobiHoc '03, New York, NY, USA: ACM; 2003, p. 153–64. http://dx.doi.org/10.1145/778415.778434.

[36] Baccelli F, Blaszczyszyn B, Muhlethaler P. An aloha protocol for multihop mobile wireless networks. IEEE Trans Inform Theory 2006;52(2):421–36. http://dx.doi.org/10.1109/TIT.2005.862098.

[37] Yang X, de Veciana G. Inducing multiscale clustering using multistage MAC contention in CDMA ad hoc networks. IEEE/ACM Trans Netw 2007;15(6):1387–400. http://dx.doi.org/10.1109/TNET.2007.902690.

[38] Ieee standard for information technology–local and metropolitan area networks– specific requirements– part 11: Wireless LAN medium access control (MAC) and physical layer (PHY) specifications amendment 8: IEEE 802.11 wireless network management. In: IEEE Std 802.11v-2011 (amendment to IEEE Std 802.11-2007 as amended By IEEE Std 802.11k-2008, IEEE Std 802.11r-2008, IEEE Std 802.11y-2008, IEEE Std 802.11w-2009, IEEE Std 802.11n-2009, IEEE Std 802.11p-2010, and IEEE Std 802.11z-2010). 2011, p. 1–433. http://dx.doi.org/10.1109/IEEESTD.2011.5716530.

[39] Hasan A, Andrews JG. The guard zone in wireless ad hoc networks. IEEE Trans Wireless Commun 2007;6(3):897–906. http://dx.doi.org/10.1109/TWC.2007.04793.

[40] Gupta P, Kumar PR. The capacity of wireless networks. IEEE Trans Inform Theory 2000;46(2):388–404. http://dx.doi.org/10.1109/18.825799.

[41] Al-Hourani A, Haenggi M. Performance of next-generation cellular networks guarded with frequency Reuse distance. IEEE Trans Commun 2019;67(10):7277–87. http://dx.doi.org/10.1109/TCOMM.2019.2930509.

[42] Feng K, Haenggi M. On the location-dependent SIR gain in cellular networks. IEEE Wirel Commun Lett 2019;8(3):777–80. http://dx.doi.org/10.1109/LWC.2019.2892422.

[43] Afshang M, Saha C, Dhillon HS. Nearest-neighbor and contact distance distributions for Thomas cluster process. IEEE Wirel Commun Lett 2017;6(1):130–3. http://dx.doi.org/10.1109/LWC.2016.2641935.

[44] Afshang M, Saha C, Dhillon HS. Nearest-neighbor and contact distance distributions for Matérn cluster process. IEEE Commun Lett 2017;21(12):2686–9. http://dx.doi.org/10.1109/LCOMM.2017.2747510.

[45] Weber SP, Yang X, Andrews JG, de Veciana G. Transmission capacity of wireless ad hoc networks with outage constraints. IEEE Trans Inform Theory 2005;51(12):4091–102. http://dx.doi.org/10.1109/TIT.2005.858939.

[46] Choudhary G, Sharma V, You I. Sustainable and secure trajectories for the military internet of drones (IoD) through an efficient medium access control (MAC) protocol. Comput Electr Eng 2019;74:59–73. http://dx.doi.org/10.1016/j.compeleceng.2019.01.007.

[47] Khan MA, Qureshi IM, Khan IU, Nasim A, Javed U, Khan W. On the performance of flying ad-hoc networks (FANETs) with directional antennas. In: 2018 5th international multi-topic ICT conference (IMTIC). MUET, Pakistan; 2018, p. 1–8. http://dx.doi.org/10.1109/IMTIC.2018.8467274.

[48] Song Y, Qi W, Zhao W. Adaptive range-based efficient spatial reuse MAC mechanism in wireless full-duplex ad hoc networks. In: 2018 IEEE international conference on communications (ICC). 2018, p. 1–7. http://dx.doi.org/10.1109/ICC.2018.8422708.
[49] Wilhelmi F, Cano C, Neu G, Bellalta B, Jonsson A, Barrachina-Muñoz S. Collaborative spatial Reuse in wireless networks via selfish multi-armed bandits. Ad Hoc Networks 2019;88:129–41. http://dx.doi.org/10.1016/j.adhoc.2019.01.006.
[50] Lu S, Wang Z. Spatial transmitter density allocation for frequency-selective wireless ad hoc networks. IEEE Trans Wireless Commun 2019;18(1):473–86. http://dx.doi.org/10.1109/TWC.2018.2881707.
[51] Sousa ES, Silvester J. ''Optimum transmission ranges in a direct-sequence spread-spectrum multihop packet radio network''. IEEE J Sel Areas Commun 1990;vol. 8(4):762–71.
[52] Aljuaid M, Yanikomeroglu H. Investigating the Gaussian convergence of the distribution of the aggregate interference power in large wireless networks. IEEE Trans Veh Technol 2010;59(9):4418–24. http://dx.doi.org/10.1109/TVT.2010.2067452.
[53] Fazil A, Hasan A, Qureshi IM, Shafi Q. Proactive channel access scheme for wireless ad hoc networks. IET Commun 2019;13(13):1893–901. http://dx.doi.org/10.1049/iet-com.2018.6191.
[54] Foschini GJ, Miljanic Z. ''A simple distributed autonomous power control algorithm and its convergence''. IEEE Trans Veh Technol 1993;641–6.
[55] Zander J. Performance of optimum transmitter power control in cellular radio systems. IEEE Trans Veh Technol 1992;41(1):57–62. http://dx.doi.org/10.1109/25.120145.

Adnan Fazil received BE in Avionic Engineering from the College of Aeronautical Engineering (CAE), NUST, Pakistan. Received MS and PhD in wireless communications from Air University, Pakistan. He has more than 13 years of experience in academics and research, and currently serving as Assistant Professor at Air University. His research interests include Wireless Ad Hoc Networks, Transmission Scheduling and applications of Machine Learning.

Aamir Hasan received BE in Avionic Engineering from CAE, and M.S. in electrical and computer engineering from University of Southern California, USA. His Ph.D. is in wireless communications from University of Texas at Austin, USA. He has over 30 years of experience in R&D and teaching, and working as an Associate Professor at Habib University, Karachi, Pakistan. His research interests are interference suppression techniques, physical layer design, spread spectrum and capacity of ad hoc networks.

Bahman R. Alyaei is serving as Assistant Professor at Electrical and Computer Engineering Department, Air University, Pakistan, since 2014. He received BSc. in communications engineering from Ajman University, Ajman, UAE, in 2002 and MS. in electrical engineering from Air University, Islamabad in 2011. He is currently pursuing PhD from Isra University, Pakistan. His current research interests include heterogeneous cellular networks.

Khurram Khan received the B.S. degree in computer engineering from COMSATS University, Pakistan, in 2007. He received the M.S. and Ph.D. degrees in electronic and communication engineering from Hanyang University, South Korea, in 2010 and 2019, respectively. Currently, he is with the Department of Avionics Engineering, Air University, Islamabad, Pakistan. His research interests include computer vision, machine/deep learning and ad hoc networks.

Muhammad Zakwan received the B.S. in electrical engineering from Air University, Pakistan, the M.S. degree in communication and information systems from Northwestern Polytechnic University, China, and the Ph.D. degree in electrical and electronics engineering from Koç University, Turkey. He is currently appointed as an Assistant Professor at Air University. His research interests include silicon photonic integrated circuits (SiPIC), communication systems and artificial intelligence.